ELSEVIER

Contents lists available at ScienceDirect

Physics Letters B

www.elsevier.com/locate/physletb



Search for photon-photon elastic scattering in the X-ray region



T. Inada ^{a,*}, T. Yamaji ^{a,*}, S. Adachi ^a, T. Namba ^b, S. Asai ^a, T. Kobayashi ^b, K. Tamasaku ^c, Y. Tanaka ^c, Y. Inubushi ^c, K. Sawada ^c, M. Yabashi ^c, T. Ishikawa ^c

- a Department of Physics, Graduate School of Science, The University of Tokyo, 7-3-1 Hongo, Bunkyo, Tokyo 113-0033, Japan
- b International Center for Elementary Particle Physics, The University of Tokyo, 7-3-1 Hongo, Bunkyo, Tokyo 113-0033, Japan
- ^c RIKEN SPring-8 Center, 1-1-1 Kouto, Sayo-cho, Sayo-gun, Hyogo 679-5148, Japan

ARTICLE INFO

Article history: Received 11 March 2014 Received in revised form 24 March 2014 Accepted 27 March 2014 Available online 2 April 2014 Editor: W.-D. Schlatter

ABSTRACT

We report the first results of a search for real photon–photon scattering using X rays. A novel system is developed to split and collide X-ray pulses by applying interferometric techniques. A total of 6.5×10^5 pulses (each containing about 10^{11} photons) from an X-ray Free-Electron Laser are injected into the system. No scattered events are observed, and an upper limit of 1.7×10^{-24} m² (95% C.L.) is obtained on the photon–photon elastic scattering cross section at 6.5 keV.

© 2014 The Authors. Published by Elsevier B.V. This is an open access article under the CC BY license (http://creativecommons.org/licenses/by/3.0/). Funded by SCOAP³.

1. Introduction

Photon–photon $(\gamma - \gamma)$ scattering is a pure quantum-electrodynamical (QED) process, in which the box diagram with an electron gives the leading-order contribution. This QED process was predicted in 1933 [1] as a characteristic effect of the non-linearity of the quantum vacuum. Although indirect tests have been performed using Delbrück scattering [2], $\gamma - \gamma$ scattering of real photons has not yet been directly observed. The direct observation of this process would provide solid evidence for vacuum polarization caused by virtual electrons, and is considered an ultimate test of OED.

In the past, visible lasers have been used to search for real $\gamma - \gamma$ scattering [3,4]. At low energies ($\hbar\omega \ll m_{\rm e}c^2$), however, the QED cross section of $\gamma - \gamma$ scattering is suppressed by the sixth power of the ratio $\hbar\omega/m_{\rm e}c^2$, where ω is the photon energy and $m_{\rm e}$ the electron mass [5]. A significant enhancement of the cross section can be obtained by using higher-energy photons, for example, X rays.

In addition to the context of QED tests, studies in a different energy region are important for the search for new physics beyond the Standard Model. A theoretical benchmark for such processes is s-channel production of light pseudoscalar bosons, namely axions [6]. If axions exist with a mass in the X-ray region, invisible axion models [7] predict that $\gamma - \gamma$ scattering is dominated by the contribution from axions under a resonant condition [8].

In this paper we report the first results of a direct search for $\gamma - \gamma$ scattering in the X-ray region. Our experiment is performed

at the SPring-8 Angstrom Compact Free-Electron Laser [9] (SACLA), an X-ray Free-Electron Laser (XFEL) which provides one of the world's most brilliant X-ray sources. To ensure the collision of $\gamma - \gamma$ in both space and time, a high-precision collision system is developed, using a single silicon crystal to split and collide X-ray pulses.

The differential cross section of the scattering of two photons with the same linear polarization is [5]

$$\left(\frac{\mathrm{d}\sigma_{\gamma\gamma\to\gamma\gamma}}{\mathrm{d}\Omega}\right)_{\mathrm{QED}} = \frac{\alpha^4 \omega_{\mathrm{CMS}}^6}{(180\pi)^2 m_{\mathrm{e}}^8} \left(260\cos^4\phi + 328\cos^2\phi + 580\right), \tag{1}$$

where α is the fine structure constant and ϕ is the scattering angle in the center of mass system (CMS). The CMS photon energy (ω_{CMS}) is 6.5 keV in our system, giving a cross section around 23 orders of magnitude larger than that at 1 eV, the typical energy of visible lasers.

2. Experimental setup

Fig. 1 shows a schematic view of the experimental setup. A pulsed beam of synchrotron radiation (repetition rate of 20 Hz) is produced in the BL(beamline)-3 of the SACLA facility (total length of 700 m), which is mainly composed of a low-emittance electron gun, C-band high gradient accelerators, and nineteen undulators. Electron beam energy and vertical gaps in the undulator magnets are tuned to produce X rays with an energy of $\omega_0 = 10.985$ keV. The pulse length of the beam is measured to be less than 10 fs [10], and each pulse contains about 10^{11} photons.

^{*} Corresponding authors.

E-mail addresses: tinada@icepp.s.u-tokyo.ac.jp (T. Inada),
yamaji@icepp.s.u-tokyo.ac.jp (T. Yamaji).

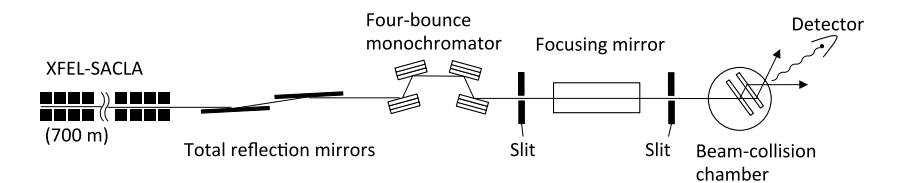


Fig. 1. Side view of the beamline components.

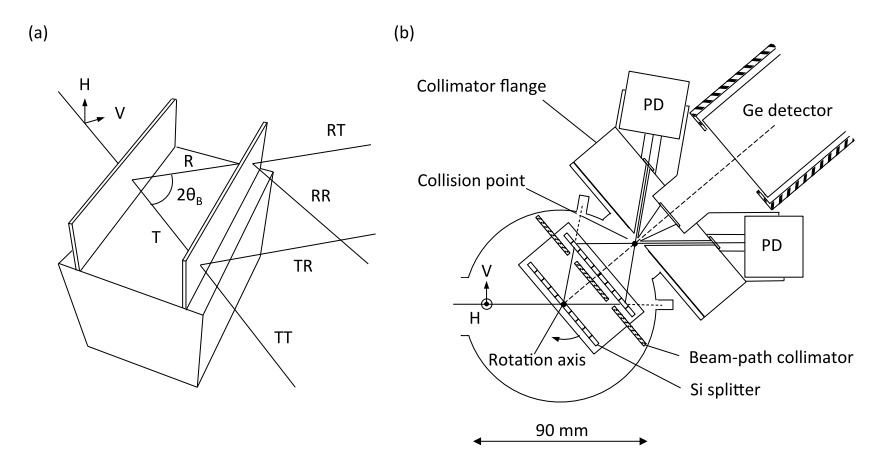


Fig. 2. (a) Four beams after the two blades of the silicon beam splitter. Horizontal (H) and vertical (V) directions are shown in a plane which is normal to the beam axis. (b) Magnified view of the beam-collision chamber.

The beam from the undulator is linearly polarized in the horizontal direction.

Higher harmonics of the X-ray beam are contained in the beam after the undulators. These higher components are removed by a pair of carbon-coated mirrors [11] placed in an optics hutch downstream of an undulator building. Their glancing angle is set to 2.0 mrad to give total reflection of X rays with an energy below 11 keV. The angle of both mirrors are the same, giving parallel incoming and outgoing beams.

The energy spectrum of the beam after the undulators has a bandwidth of about 50 eV. The monochromaticity is improved to the level of ~ 60 meV (FWHM) by a four-bounce monochromator with silicon (440) reflection, placed downstream of the total reflection mirrors. The beams are reflected and filtered in energy with the Bragg condition at the first surface. The second one is used to change the beam axis. The same mechanism is used in a second pair of silicon surfaces, restoring the vertical offset of the beam axis.

The horizontal beam size is focused from $\sim 200~\mu m$ to $\sim 1~\mu m$ by an elliptical focusing mirror (focusing length =1.5 m, Rayleigh length $\sim 10~mm)$ [12]. The vertical direction is not focused and remains at its original size ($\sim 200~\mu m$), since the vertical component of the beam contributes to the Bragg reflection at the silicon splitter. The spatial beam profile has a Gaussian distribution. In order to improve the beam quality, a pair of four-jar slits is inserted along the beam axis, on either side of the focusing mirror. These slits are used to block the side-lobes of the beam and diffuse scattering from the mirror.

An X-ray interferometer technique [13] is applied to split and collide X-ray pulses. A schematic view of the beam splitter is shown in Fig. 2a. The collision of the beams is assured by the geometrical equivalence of the beam paths split by symmetric Laue reflection [14]. The beams are split and collided by two 0.6 mmthick blades of (440) silicon crystal cut from a high-quality single crystal. The blades are separated by 25 mm. A magnified view of the beam-collision chamber is shown in Fig. 2b. The two blades are placed so as to split and collide X rays in a vertical-longitudinal

plane; this geometry minimizes the loss of the π -polarized component. The blades are installed in a cylindrical vacuum chamber (beam-collision chamber) and fixed to a rotary feedthrough connected to a goniometer. The center of the first blade is aligned to coincide with the rotation axis of the goniometer. The rotation angle of the lattice plane (θ_B) is tuned to satisfy the condition for Laue reflection.

The incident beams are split into two coherent beams at the first blade; one is the transmitted beam (T) and the other is the reflected one (R), with a reflection angle of $2\theta_B = 72^\circ$ (Fig. 2a). A similar process occurs at the second blade, creating four beams after the two blades. Two beams (TT and RT) are dumped into pits on the wall of the chamber. The other beams (TR and RR) collide at a collision point and pass through a vacuum window made of 125 µm-thick polyimide. The collision point is adjusted to be at the focusing point of the mirror. The intensities of the two beams are monitored pulse-by-pulse by silicon PIN photodiodes (PDs, HAMAMATSU S3590-09), inserted in stainless steel holders fixed to the chamber flange and wrapped in a 3 mm-thick lead sheet to avoid photon leakage. In order to reduce X rays scattered by air, the beam path is evacuated upstream of the collision chamber (< 10^{-5} Pa) and inside the chamber (< 10^{-2} Pa).

The TR and RR beams collide obliquely with a crossing angle of $2\theta_{\rm B}$. The CMS energy of each photon is $\omega_0 \sin \theta_{\rm B}$ and the two-photon system is boosted with an energy of $2\omega_0 \cos \theta_{\rm B}$. The maximum and minimum energies of scattered photons, given by $\omega_0(1\pm\cos\theta_{\rm B})$, occur for photons scattered along the boost axis. Since forward-scattered photons have higher energy than the original photons, it is easy to separate their signal from backgrounds. To select forward-scattered photons, a collimator flange with a conically tapered hole is placed after the collision point. The full angle of the cone is 25°, defining the signal energy region from 18.1 keV to 19.9 keV. A second beam-path collimator (stainless steel, thickness = 2 mm) with two holes (diameter = 6 mm) is inserted between the two blades. The two beams from the first blade pass through the collimator, while Rayleigh- or Compton-scattered photons from the blade are blocked.

Download English Version:

https://daneshyari.com/en/article/1853108

Download Persian Version:

https://daneshyari.com/article/1853108

Daneshyari.com